NANO · MICRO small
www.small-journal.com

Transport Phenomena in Zeolites in View of Graph Theory and Pseudo-Phase Transition

*Dali Cai, Hao Xiong, Chenxi Zhang, and Fei Wei**

Transport phenomena play an essential role in catalysis. While zeolite catalysis is widely applied in industrial chemical processes, its efficiency is often limited by the transport rate in the micropores of the zeolite. Experimental and theoretical methods are useful for understanding the transport phenomena on multiscale levels. Traditional diffusion models usually use a linear driving force and an isotropic continuum medium, such that transport in a hierarchical catalyst structure and the occurrence of nonlinear deactivation cannot be well understood. Due to the presence of spatial confinement and an ordered structure, some aspects of the transport in a zeolite cannot be regarded as continuum phenomena and discrete models are being developed to explain these. Graph theory and small-world networks are powerful tools that have allowed pseudo-phase transition phenomena and other nontrivial relationships to be clearly revealed. Discrete models that include graph theory can build a bridge between microscopic quantum physics and macroscopic catalyst engineering in both the space and time scales. For a fuller understanding of transport phenomena in diverse fields, several theoretical methods need to be combined for a comprehensive multiscale analysis.

1. Introduction

Zeolites, which are also known as molecular sieves, are ordered porous materials with wide usage.[1] They are widely used in the coal-to-chemicals,[2–4] petrochemical[5,6] and environmental industries[7–9] for gas separation,[10,11] adsorption, and catalysis.[12] Zeolite catalysis is an imperative part of heterogeneous catalysis and the chemical industry.

Making catalysts with high selectivity, conversion, and long lifetime has been the purpose of catalysis researchers, where diffusion and deactivation issues have been the important barriers to overcome. During a reaction, the diffusion of molecules in zeolite crystals significantly influences performance and product distribution. A focus on this diffusion has driven much development work in catalyst engineering. Numerous methods have been developed to synthesize nanosized zeolites and hierarchical zeolites to enhance diffusion. A parallel phenomenon, coking, which is the primary cause of the deactivation of zeolite catalysts, leads to pore blockage in the zeolite and adversely affects diffusion rates, and also wastes feedstock and lowers atom efficiency. The suppression of coke formation is also a central topic in catalysis.

Traditional kinetic studies regard catalyst pellets as isotropic and describe diffusion with a lumped diffusion coefficient, although in Monte Carlo studies, the zeolite topology is used, and models based on zeolite topology and network are built and the strong coupling of diffusion and deactivation is analyzed. As a complement to these, it is expected that in modern transport research, more use will be made of discrete models. Some exciting new findings from these include pseudo-phase transition phenomena noted in the deactivation process and the fast transport in nanosized channels and hierarchical catalyst structure. In this review, we seek to provide insights on zeolite diffusion studies from the traditional view to modern discrete models.

Dr. D. Cai, H. Xiong, Dr. C. Zhang, Prof. F. Wei
Beijing Key Laboratory of Green Reaction Engineering and Technology
Department of Chemical Engineering
Tsinghua University
Beijing, China
E-mail: wf-dce@tsinghua.edu.cn

The ORCID identification number(s) for the author(s) of this article can be found under https://doi.org/10.1002/smll.201901979.

DOI: 10.1002/smll.201901979

2. Traditional Methods of Studying Diffusion and Deactivation in Zeolites

2.1. Experimental Methods for Diffusion and Deactivation Measurement with Zeolites

Measuring the diffusion coefficient experimentally is an essential first step, and various methods have been developed for this. Uptake methods obtain the diffusion coefficient by the measurement of adsorption or desorption amount versus time.[13] While assuming a consistent surface concentration and a uniform diffusion coefficient D_T, the molecular uptake can be fitted by the formula ($M(t)$ is for molecular uptake at specific time t, R is for estimated particle size)

$$\frac{M(t)}{M(\infty)} = 1 - \frac{6}{\pi^2}\sum_{n=1}^{\infty}\frac{1}{n^2}\exp\left(-\frac{n^2\pi^2 D_T t}{R^2}\right)$$

Thus, by curve fitting, the average diffusion coefficient is calculated. However, this method needs an estimated particle size, but this is not well defined in most cases.

The zero length column (ZLC) method was developed to avoid external heat and mass transport limitation.[14] While the use of chromatography provides higher precision, other spectroscopic methods are also used to measure the concentration, either in the zeolite crystals or the gas phase, for the diffusion measurement.[15,16]

Neutron scattering is a powerful tool for transport study. Herve´ Jobic et al. reported the combination of neutron scattering and molecular simulation to study transport phenomena.[17,18] Diffusion of different molecules including methane, n-butane, etc. over zeolites (Silicalite-1) are studied. Maurin and coworkers reported the diffusion study of CO_2 in metal-organic framework (MOF) materials with Neutron scattering.[19] Due to the interactions between CO_2 molecules, it does not behave like ideal gas. Catlow et al. studied methanol diffusion in zeolite HY with quasi-elastic neutron scattering, which can hardly be done by other methods due to the reactivity of methanol and crystal size.[20]

Wei and coworkers measured xylene diffusion over ZSM-5.[21] p-Xylene has a larger diffusion coefficient than the other two xylene isomers. However, the diffusion phenomenon becomes complicated when some part of the zeolite channels are also occupied by molecules. Kolvenbach et al. measured i-butane diffusion over normal-sized ZSM-5 crystals and a large ZSM-5 single crystal. They showed that the ZSM-5 single crystal gave a faster diffusion and no uneven distribution was found in it. Lercher and coworkers reported the diffusion of C_4 alkanes in nanosized ZSM-5.[22] They indicated that the diffusion rate of the alkane mixture was limited by the pore entry step. Wei and coworkers reported a diffusion measurement of ethane and propane over SAPO-34 zeolite and noted the difference between the diffusion rates of ethane and propane.[23] Ethane diffusion is almost not influenced by crystal size and coke percentage, while propane is.

Concerning the deactivation process, coke accumulation often plays a critical role in deactivation influenced by the diffusion of the effluents. For studying this aspect, many methods are used in resolving the kinetics and reaction pathways. Guisnet et al. gave a general review in 1989 of the method that used HF solution to dissolve the framework of zeolite and used CH_2Cl_2 to extract aromatic species with up to four aromatic rings for analysis.[24] This has become a standard method for the analysis in zeolite catalysis. Weckhuysen and coworkers have developed a series of in situ methods for analyzing coke with in situ spectroscopy.[25–33]

2.2. Theoretical Analysis and Modeling for Diffusion Phenomena

Experimental results are complicated by that the diffusion coefficient is influenced by the zeolite structure, molecular structure, concentration, pore occupation, and the probable strong coupling of diffusion and deactivation.[28,34] The measured average diffusion coefficient is actually a lumped parameter that cannot give detailed information. Due to this, models have been developed to give a microscopic picture of diffusion, which may include deactivation as both a contributing cause and effect.

Dali Cai received his B.E. and Ph.D. degrees from Tsinghua University in 2014 and 2019. His research focuses on zeolite structure theory and catalysis in the methanol to olefin/aromatics process.

Chenxi Zhang is now a postdoctoral fellow in Prof. Fei Wei's group. He received his B.E. from Tongji University in 2013, and his Ph.D. from Tsinghua University in 2017. His research focuses on stability of uniform gas solids flow, mechanisms of phase separation in gas solids flow, Fluidized Catalytic Cracking (FCC) in downer reactors, and countercurrent multistage cyclonic reactors.

Fei Wei received his Ph.D. degree from China University of Petroleum in 1990 and has been a full professor in Tsinghua University since 1996. His research interests include synthesis and properties of carbon nanotube and other carbon materials, energy storage materials, zeolite catalysis engineering for methanol/syngas conversion, and mechanisms in gas solids flow.

In earlier works, the zeolite was regarded as a porous media and traditional models of mass transfer in reaction engineering were applied.[35,36] Froment and coworkers constructed percolation models and applied them to the butene oxidative dehydrogenation reaction.[37] Sahimi gave insights into the power law relationship in diffusion over disordered porous media based on a Bethe network.[38]

Molecular dynamics (MD) is also usually used in diffusion studies of zeolites. Leslie and coworkers constructed an MD model for methane and ethylene diffusion in ZSM-5 zeolites (**Figure 1**).[39] Krishna and coworkers gave insights on the diffusion coefficient of different gases and mixtures (including CH_4, CO_2, N_2, etc.) in different zeolite structures (including

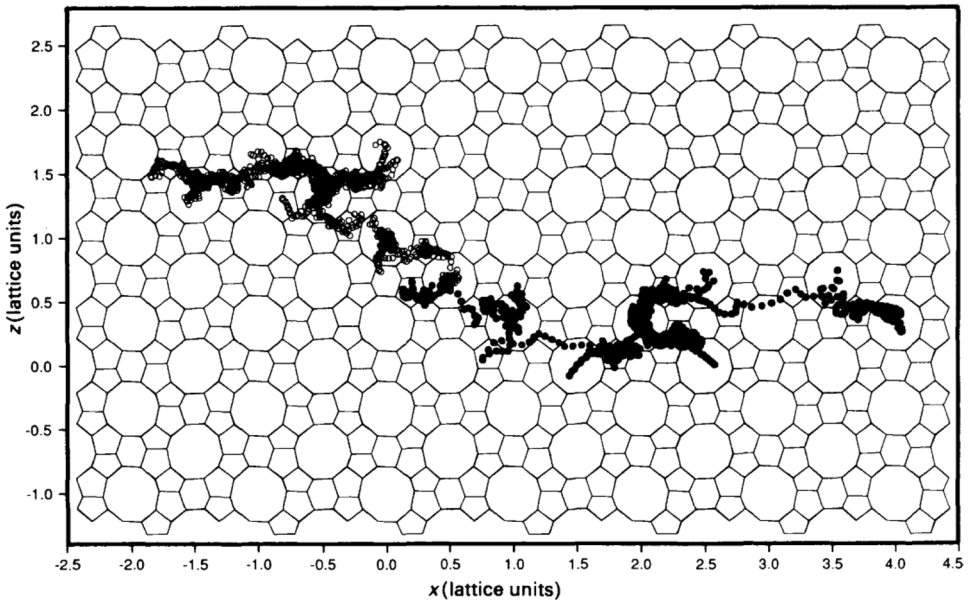

Figure 1. Two methane molecules diffuse in ZSM-5. Reproduced with permission.[39] Copyright 1991, RSC Publications.

MFI, CHA, FAU, etc.).[40] They reported that the diffusion coefficient dramatically increased with the increase of gas loading. For zeolites with cages that have small pore openings, e.g., the CHA type, it is diffusion through the small windows that is difficult, and the diffusion coefficient is limited by this. Xie and coworkers studied the diffusion of light olefins, e.g., ethylene and propylene, over different zeolite structures including CHA, MFI, FAU, etc.[41] The diffusion of propylene is restricted in CHA type zeolite by the small cage windows.[42] This gave an essential understanding of the selectivity in the methanol-to-olefins process. Berend Smit and coworkers reviewed the Molecular simulations in transport study.[43]

Besides MD, more physical models have been developed. A random walk model was applied to study diffusion in MFI zeolites by Kärger et al. (**Figure 2**).[44] An anisotropic diffusion coefficient was shown by methane diffusion in ZSM-5 zeolite. Kärger and coworkers have also done much work on diffusion in MOFs and other nanomaterials.[45–47] Hashimoto and coworkers further developed the random walk model and applied it to more zeolites with different topology.[48] Experimental results from NaY zeolite were compared with the model.

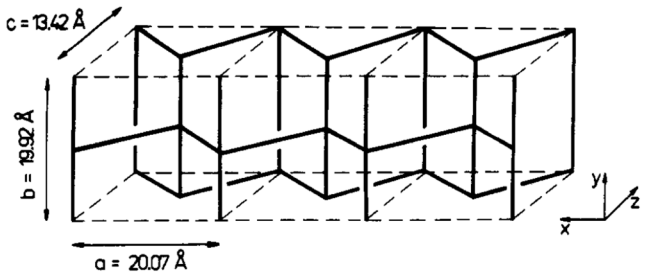

Figure 2. Random walk model for the MFI structure. Reproduced with permission.[44] Copyright 1991, ACS Publications.

The stochastic Monte Carlo method, as a common method in calculation and simulation, has been applied in diffusion calculation in zeolites. Smith et al. calculated the Knudsen diffusion coefficient in restricting pores in zeolites with the Monte Carlo method.[49] Guo et al. reported a Monte Carlo simulation for coke deposition in zeolite channels.[50] The relationship between coke content and time and pressure was studied.

Based on these results, ordered network models were established according to the zeolite topology. Rajagopal et al. developed network structure models for different zeolites, including MFI, FAU, etc., and from the investigation of these network models, the significance of the network structure was developed. Golshan and coworkers also gave a network model for catalyst pellets.[51]

3. Analyzing Diffusion and Deactivation with Graph-Based Discrete Models

3.1. Graph Theory and Other Discrete Models

Modeling is essential in studies of diffusion in zeolites. Previous models cannot access many details in the phenomena for they cannot include the important topology and its fluctuating during the reaction. For example, a sudden change in conversion with time cannot be adequately interpreted with these models.

For an ordered zeolite network, graph theory is a powerful tool for analyzing it. A graph (in the graph theory sense) can be used to elucidate the connection between elements, which is essential in transportation. Erdős and Rényi have established a random network model (known as the Erdős–Rényi model)[52,53] with which a pseudo-phase transition phenomenon was noted, namely, there is a critical probability p_c that determines the connectivity of the graph.

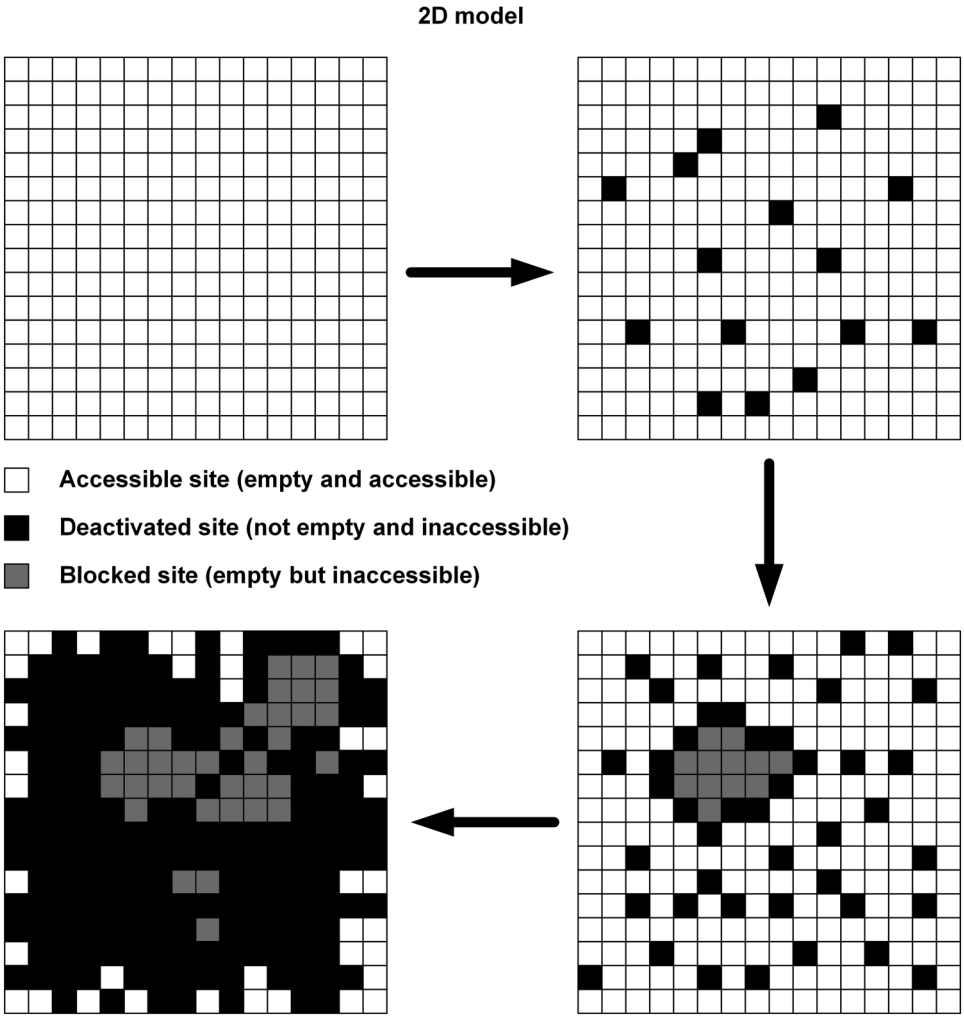

Figure 3. Illustration with a 2D case. Reproduced with permission.[58] Copyright 2017, RSC Publications.

Some other models also gave a phase transition. The Ising model, as another discrete model of importance, can explain phase transition in two and more dimensions. There is also generalized phase transition phenomena noticed in the percolation model[37,54–57] and in Go.

3.2. Pseudo-Phase Transition Phenomenon Shows Similarity to the Go Game

By regarding the ordered zeolite structure as a graph, we can build a discrete model that illustrates nonlinear deactivation phenomena.[58] The cages in the zeolite are regarded as nodes and channels as edges. Some underlying assumptions are that deactivation only occurs at acid cages stochastically and individually, and after the accumulation of coke in a particular cage, all its neighbors would be disconnected.

Figure 3 gives a demonstration for the 2D case. All cages have acidity. Each square represents a cage, and each cage has four neighbors. With increasing time, coke sites appear (represented with black squares), and their cages lose their connection to other sites. However, there also appears another type of sites (represented with grey squares), which are not coked, but because they are surrounded and blocked by coke sites, so from an external view, they are regarded as deactivated sites. This is similar to what happens in Go, where some stones lose their connection to the outside (called liberty in Go) and have to be removed. These cages that are blocked but not deactivated lead to the nonlinear change of conversion in the zeolite. A pseudo-phase transition phenomenon has occurred.

For the simplest case, i.e., the 1D case with all acid sites, there is an analytical solution for how the conversion changes with time.

Figure 4 gives a demonstration of the deactivation process of 1D zeolites. When there are two deactivated sites, all the sites between them are blocked. Measuring time as the number of steps m, and denoting the deactivation probability for each node in each step as p, for a model with length N, the probability that n nodes remain alive after m steps, P(n), has the formula

$$P(n)=\begin{cases} Q^N & n=N \\ N(1-Q)Q^{N-1} & n=N-1 \\ (n+1)(1-Q)^2 Q^n & 0\le n<N-1 \end{cases}$$

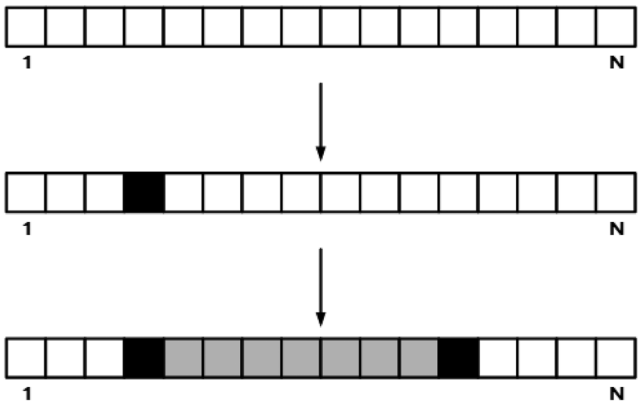

Figure 4. 1D zeolite deactivation with time. Reproduced with permission.[58] Copyright 2017, RSC Publications.

where $Q = (1 - p)^m$.

The percentage of deactivation after m steps C(m) is

$$C = \frac{\left(2Q^N - NQ^N - 2\right)Q + NQ^N}{N\left(Q-1\right)}$$

For experimental validation, the model used methanol conversion over ZSM-12. ZSM-12 is a zeolite with 12-membered rings and 1D channels.[59] Methanol conversion to heavy aromatics can be achieved over ZSM-12.[60]

Figure 5 gives the comparison between model and experimental results. With time, the conversion of methanol goes down, and the 1D analytical result can be validated by the reaction over ZSM-12. In this comparison, only the parameter of first-order kinetics is introduced, and the model with structure information can better fit the experiments.

For 3D cases, a numerical method has to be used. **Figure 6** gives a deactivation process with time. The blocked percentage was calculated. In the yellow zone in the figure, the blocked percentage suddenly increased, and this led to fast deactivation. From the visual demonstration for the 2D case, we can also get the information that at a particular time, some deactivation at a critical site will lead to the deactivation of the whole system, that is, a pseudo-phase transition phenomenon occurred.

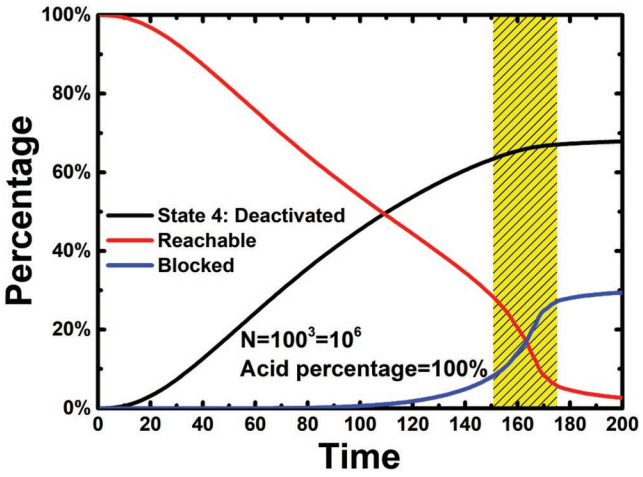

Figure 6. Deactivated percentage change with time. Reproduced with permission.[58] Copyright 2017, RSC Publications. Deactivated percentage (black line) indicates the percentage of cages (nodes) which are fully occupied by coke and deactivated. The blocked percentage indicates the percentage of cages which are empty but have lost connection to the outside. The reachable percentage indicates the percentage that is neither deactivated nor blocked.

Investigations of acid site density and its distribution are indispensable in zeolite catalysis. By using a model containing different profiles of acid distribution, useful relationships can be revealed.

Figure 7 gives the relationship between acid percentage and accessible acid percentage after some steps. For an ideal catalyst, all acid sites should be accessible. Moreover, it may seem that more acid sites would give a better catalyst performance.

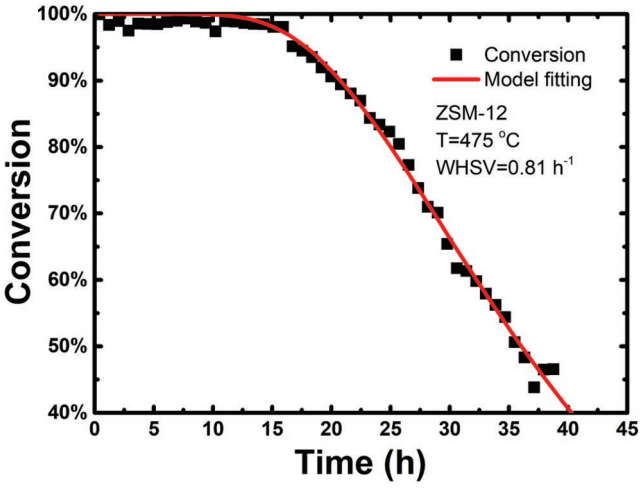

Figure 5. Methanol conversion after catalytic reaction over ZSM-12: model versus experimental results. Reproduced with permission.[58] Copyright 2017, RSC Publications, experiments are performed at $T = 475$ °C, $P = 1$ atm, WHSV = 0.81 h^{-1}, Si/Al ratio of ZSM-12 is 36.

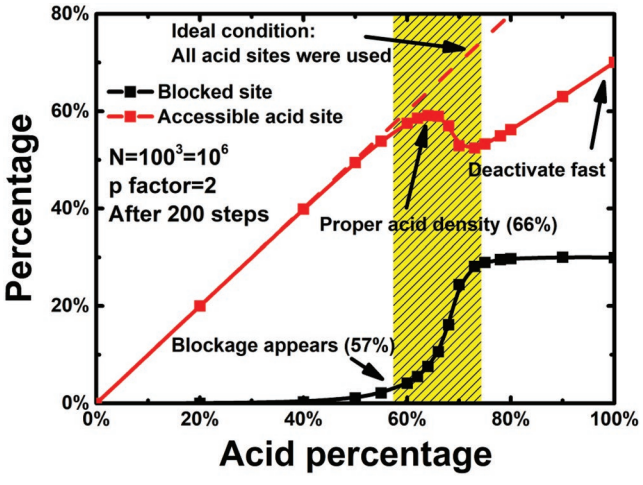

Figure 7. Impact of the acid site density. Reproduced with permission.[58] Copyright 2017, RSC Publications. The acid percentage indicates the percentage of cages that have an acid site in it. Black line indicates the blocked percentage, red line indicates the accessible acid site percentage, which equals (1-blocked percentage) × acid percentage.

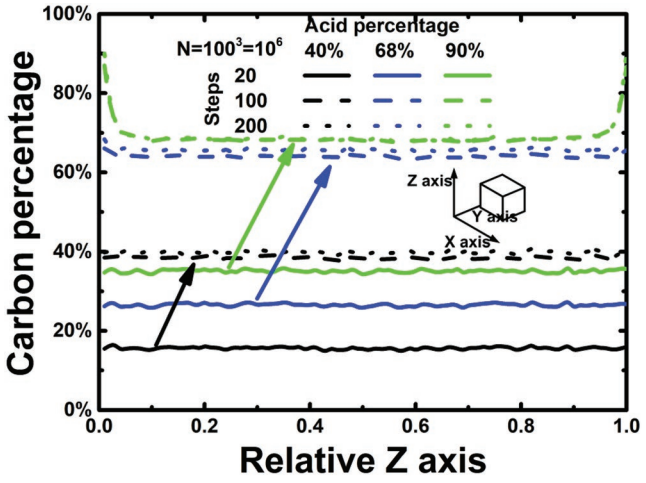

Figure 8. Coke distribution in zeolite as influenced by the acid site density. Reproduced with permission.[58] Copyright 2017, RSC Publications.

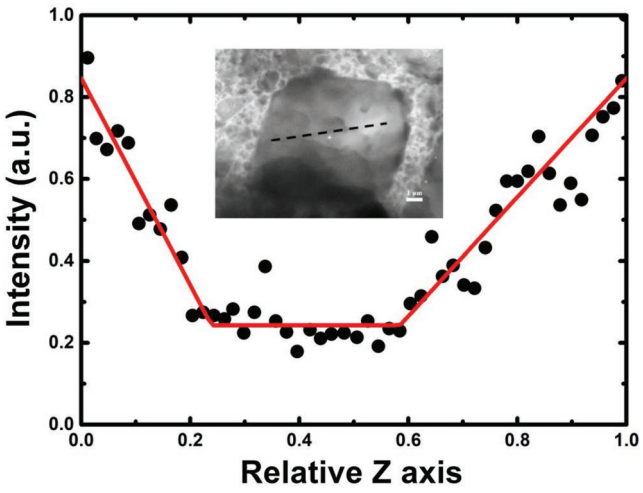

Figure 9. Experimental results for coke distribution based on energy-dispersive X-ray spectroscopy (EDS). Reproduced with permission.[58] Copyright 2017, RSC Publications, black dots indicate the intensity of Carbon signals in EDS line scanning. Red line is for the curve fitting.

However, because of "traffic jam" and the surrounding effect, some acid sites are wasted. When the acid site concentration is low, the accessible acid sites increase is synchronized with the acid sites increase. In contrast, in the range between 57% and 75%, the blocked percentage rapidly increases, leading to the consequence that the accessible percentage goes down even as the acid percentage goes up. That is, the acid sites are not efficiently used. In addition, although the accessible acid percentage is more when the acid percentage is 100%, this situation is not appropriate for the reaction because of fast deactivation. Here we reach a nontrivial result that there exists an optimal amount for the acid concentration because of the topology effect.

These discrete models can also be useful for an analysis of the shell coking effect. **Figure 8** shows the result that different concentrations of acid sites will lead to differences in coke distribution. For the case of 40% acid site percentage, the coke is evenly distributed in the zeolite. However, for a higher acid site percentage (90%), we can note that while coke is uniformly distributed at first, however, later, more coke is deposited at near-surface sites, resulting in an enriched surface coke concentration phenomenon.

Experimental results (**Figure 9**) showed that for a high acid percentage SAPO-34 zeolite, the coke distribution follows surface concentration rules. The near-surface coke layer is vital in a way described below and it should be given attention in catalyst engineering.

3.3. Transport Phenomena Analysis by Graph Theory

Discrete models that use graph theory can give us a picture of deactivation in a zeolite. Based on these, we can use the properties of the graph to gather information about transport. In order to analyze transport in the zeolite in this way, a new concept needs to be defined (**Figure 10**).[61] Latora and Marchiori reported a newly defined efficiency for analyzing transport in a network.[62] Based on this, a new index is used to probe the transport performance.

The external space is regarded as extra nodes, with one each connected to the boundary nodes. The average distance is defined as the average of the length of all shortest paths from the acid node to an external node. A deactivated node will lose all its connection to its neighborhood, as mentioned before. Moreover, for defects, all its neighborhood are regarded as connected (**Figure 11**).

The analysis of the transport property with the network is as follows. As shown in **Figure 12**, the average distance increases first and then falls. In the first stage, with the deactivation of the zeolite, acid sites are partially blocked, and the shortest length for all acid sites increased. This stage ends near the phase transition point. After this, a significant number of acid sites are blocked, and only near-surface sites are alive. In the last stage, the average distance is reduced to about one regardless of how big the network is, which indicates that only surface sites remain alive.

A small-world network is a network where the number of neighbors for each node is much smaller than the total number of nodes. A social network is a typical small-world network, for there are a large number of people in society but each of us knows just a few of them. Interestingly, the small-world network

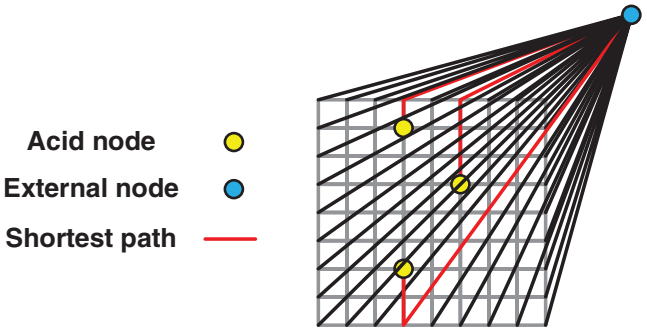

Figure 10. Definitions of average distance. Reproduced with permission.[61] Copyright 2018, RSC Publications.

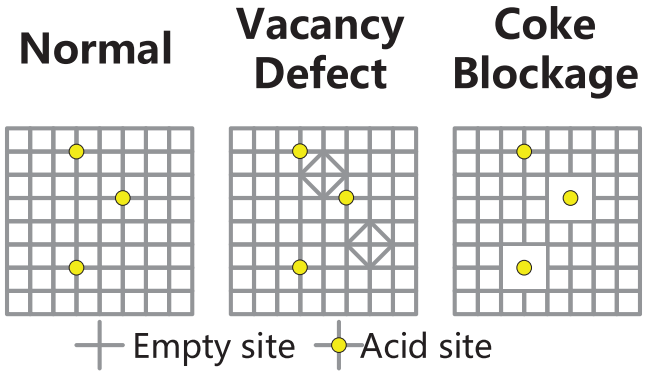

Figure 11. Definitions of coke sites and defect sites. Reproduced with permission.[61] Copyright 2018, RSC Publications.

has a superior transport efficiency; namely, the shortest length L between any two nodes is proportional to the logarithm of the total number of nodes in the network. Watts and Strogatz have developed a model[63] that indicated that a small-world network lies structurally between an ordered network and random network, and its transport efficiency comes from a small amount of long-range connection in the network.

For a perfect 3D zeolite network with 100% acid site percentage, the average distance is

$$d_{\text{average}} = \frac{(N+2)^2}{8N}$$

When N is large enough, $d_{\text{average}} \propto N$, indicating that the diffusion rate has a linear relationship with the crystal diameter. Following the same method, adding some long range interconnection, i.e., defects, will benefit transport efficiency.

Figure 13 displays the change in the average distance that is due to adding a defect into the network. When the defect concentration is lower than 1%, defects show nearly no effect on the average distance. However, the average distance falls

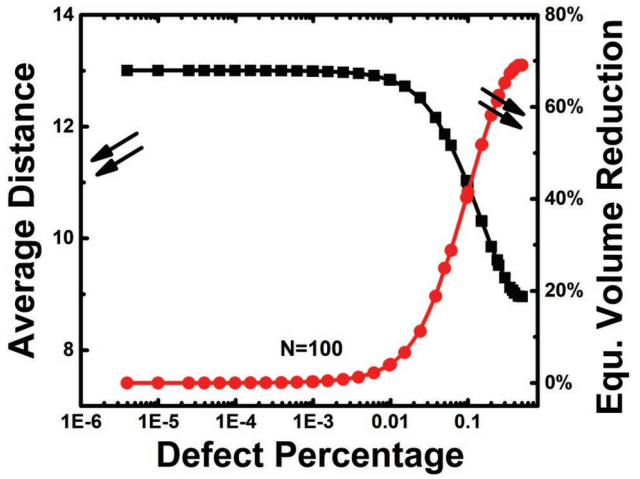

Figure 13. The relationship between the average distance and defect percentage in a $100 \times 100 \times 100$ network. Reproduced with permission.[61] Copyright 2018, RSC Publications. The black line is for average distance changing with defect percentage, and red line is for equivalent volume reduction changing with defect percentage. Equivalent volume reduction indicates the volume reduction between a perfect zeolite network, which has the same average distance as the defected one, and the defected one.

when the defect percentage is higher than 1%. With respect to the average distance, a zeolite network containing 5% defects is equivalent to a smaller particle with 22% less volume. This implies that adding defects has the same, if not better, the effect of enhancing diffusion in zeolite channels since generating defects in the zeolite instead of making nanosized zeolite crystals does not cause the problems that come with nanotechnology, e.g., the poor mechanical strength of the nanosized zeolite particles.

The spatial distribution of the acid sites also shows an influence on the average distance. The results due to different spatial distribution profiles are shown in **Figure 14**. More defects at

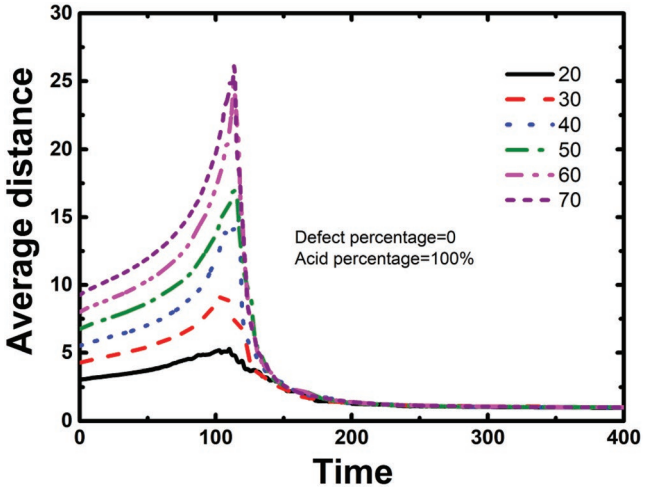

Figure 12. Change in the average distance with time for a perfect zeolite network. Reproduced with permission.[61] Copyright 2018, RSC Publications, different line for different network size (listed in the figure legend), the average distance is calculated based on the method mentioned above.

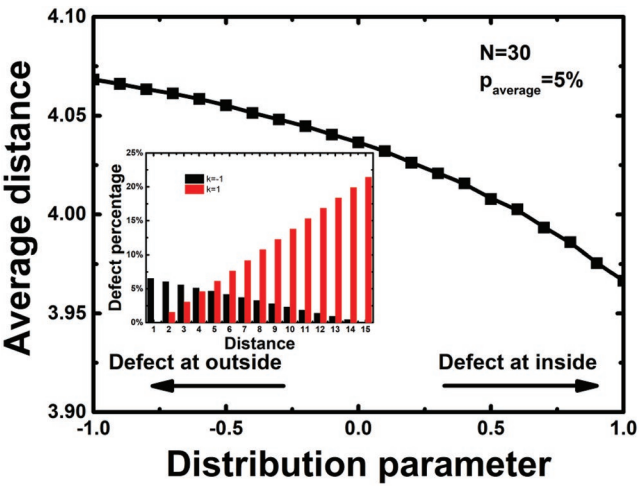

Figure 14. Influence of radial defect distribution. Reproduced with permission.[61] Copyright 2018, RSC Publications. Distribution parameter is the slope of linear distribution of defects. While the distribution parameter <0, defects is more at the outer shell, and vice versa.

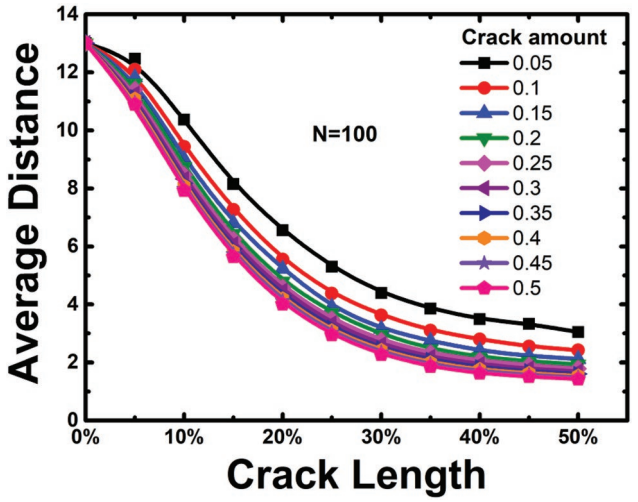

Figure 15. Influence of crack length and density for a 100 × 100 × 100 zeolite network. Reproduced with permission.[61] Copyright 2018, RSC Publications. Crack is defined as a line of defects from the zeolite surface. A different line indicates a different concentration of cracks at surface.

the outside gave a longer average distance for diffusion than defects at the inside.

Isolated vacancy defects are not effective because no long-range interconnection is built. Linear vacancy defects are the most efficient way to enhance transport efficiency, which is a situation like a small-world network with a few long channels in the form of a few long-range mailmen. **Figure 15** shows the effect. Adding long cracks into the zeolite crystal can significantly reduce the average distance; however, limited effects of increasing crack density are noticed. If these effects are combined, the superfast transport in nanochannels of water can be 1000-fold faster than normal viscous flow in a carbon nanotube or aquaporin, the total transfer efficiency can be significantly improved, that is the ideal case of superfast transport in a zeolite catalyst system. In fact, the life systems of plants and animals have such structure, like aquaporin for sweat, of a unique superfast transport mechanism. For water and blood transport, they have small and long channels for better transport performance that follows a small world network.

4. Improving Transport Efficiency by the Application of Discrete Models

4.1. Presynthesis Methods

Based on transport theory, various methods have been suggested for making hierarchical zeolite structures. The design of structure directing agents (SDAs) to achieve a good performance zeolite is an important method. Choi et al. first reported a single unit cell ZSM-5 zeolite and its excellent performance in the methanol-to-hydrocarbon reaction (**Figure 16**).[64] Since then, the design of SDAs has become vital for zeolite structure construction.

With a special designed SDA, the crystallization process can be confined, and the thickness of the zeolite crystals can be controlled. Ryoo et al. reported some more structural designs for SDAs to adjust the zeolite structure.[65] Xiao and coworkers[66,67] reported adding urea as SDAs to synthesize a kind of ZSM-5 that is 100 nm along the *b*-axis. Wei and coworkers[68] reported a short *b*-axis nanosized ZSM-5 that is 40 nm thick along the *b*-axis. A strong anisotropic transport phenomenon was noticed. Diffusion in the straight channels along the *b*-axis is 100 times faster than through the zigzag channels (**Figure 17**).[69]

Corma and coworkers reported a new method to "design" a zeolite that targets the reaction.[70] SDAs were constructed that emulated the structure of the transition state of the reaction. The synthesized zeolite exhibited excellent performance for the designated reaction. Besides SDAs, other mesopore-generation agents can be applied to generate mesopores and even macropores in zeolite crystals. Polymers are often used as the mesopore generating agent. Adding polyethylene glycol (PEG) into the synthesis of SAPO-34 will give a hierarchical structure.[71] Shen et al. reported synthesizing a macro-microporous MOF using polystyrene as a macropore generating agent (**Figure 18**).[72]

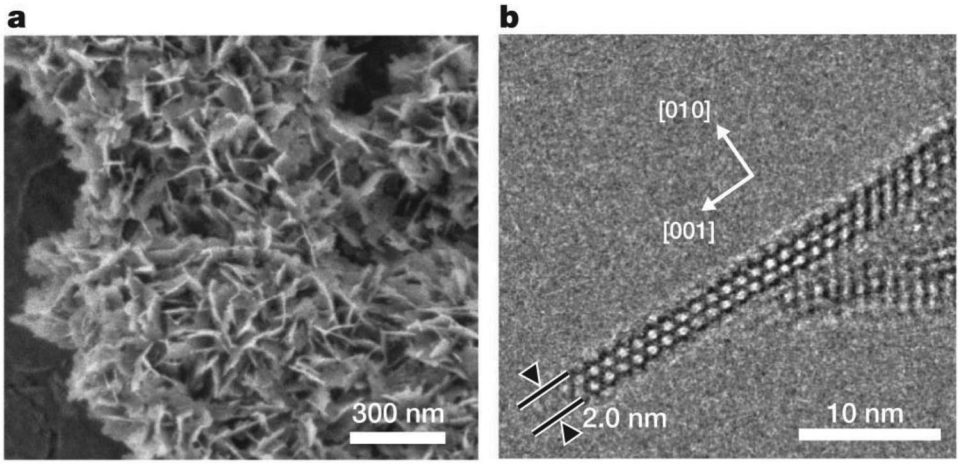

Figure 16. Structure of the single-unit-cell ZSM-5. Reproduced with permission.[64] Copyright 2009, Nature Publishing Group.

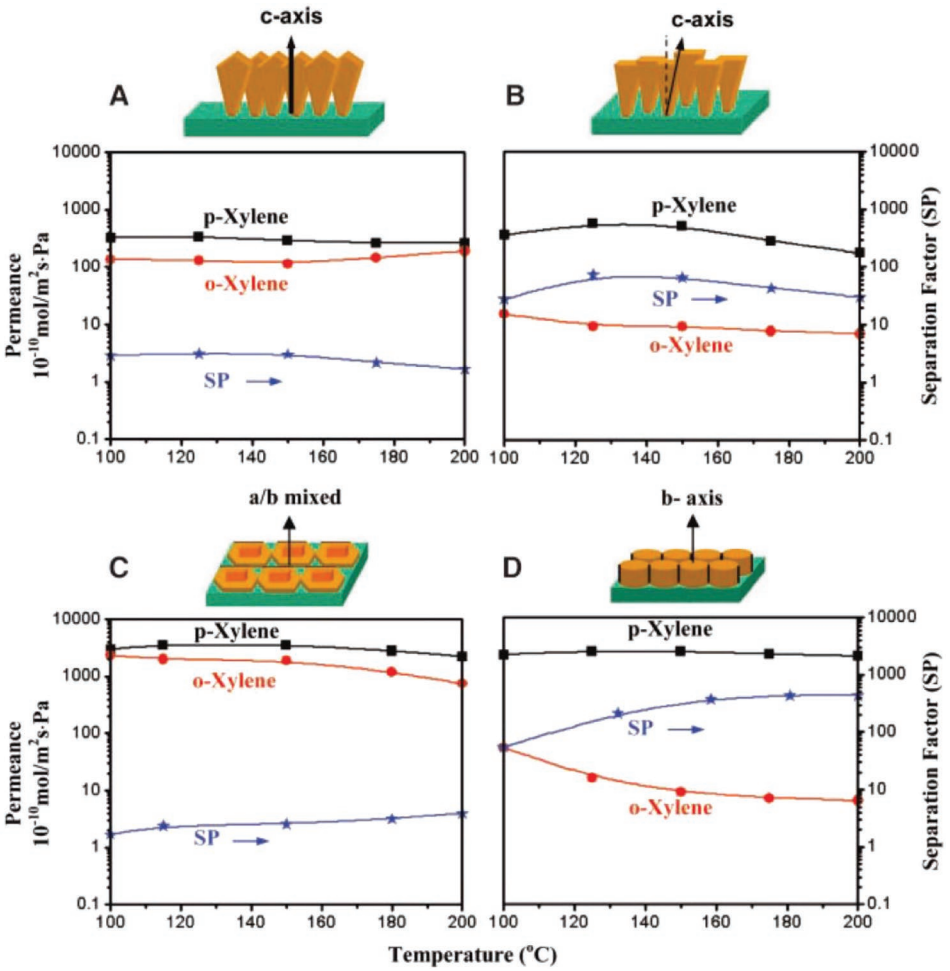

Figure 17. Different transport efficiency along different axes shows anisotropy. Reproduced with permission.[69] Copyright 2003, AAAS.

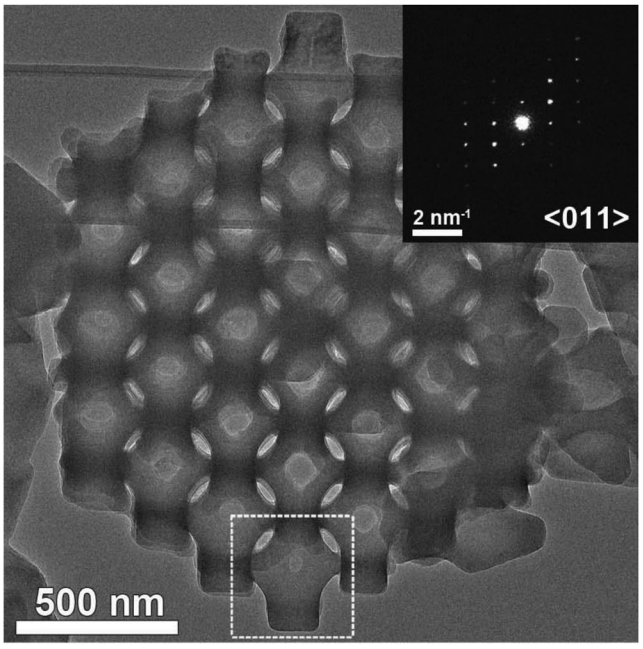

Figure 18. Ordered macro-microporous MOF structure. Reproduced with permission.[72] Copyright 2018, AAAS.

Alternative element sources for zeolite synthesis can also be used to control the structure of the synthetic zeolite. A silica source with a unique morphology can be used to build structures similar to the silica source. Using silica nanowire as the silica source can give a 1Doriented ZSM-5.[73] A silica sphere will lead to crystal growth on its surface that builds a bayberry structure.[74]

4.2. Post-Treatment and Catalyst Engineering Methods

Structural modification after synthesis is commonly used to achieve a better hierarchical structure. Acid or alkaline treatment can help the dealumination process and generate mesopores.[75–78] A fluoride ion treatment helps the reconstruction of crystal structures. Fang and coworkers used an HF treatment to enhance the catalyst lifetime in the methanol-to-hydrocarbon reaction over ZSM-5.[79] Valtchev and coworkers treated zeolite crystals with ammonium fluoride to produce a mosaic structure for improving diffusion (**Figure 19**).[80] Pérez-Ramírez and coworkers synthesized ZSM-5 crystals with different defect concentrations that helped improve performance for the 2-methyl-2-butene cracking reaction.[81]

A new methodology can be evolved in catalyst engineering to build hierarchical structures. Pereira and coworkers reported

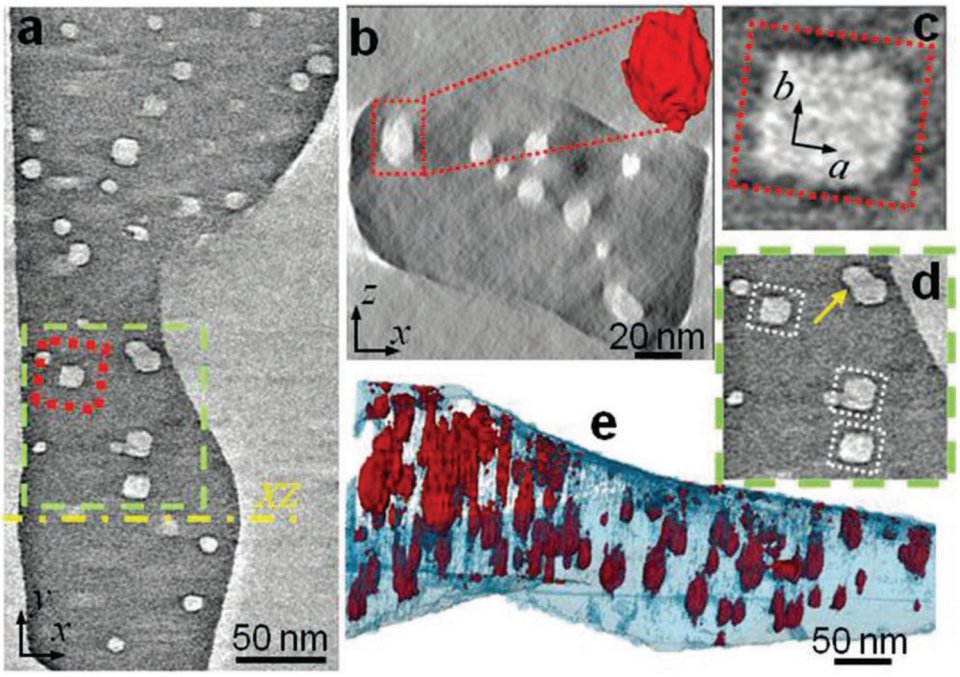

Figure 19. Generation of a mosaic structure. Reproduced with permission.[80] Copyright 2016, Wiley-VCH.

a comprehensive method including sol-gel, double-polymer template, and rapid prototyping[82] for building a hierarchical structure on multiple scales to open a new horizon for zeolite catalyst engineering (**Figure 20**).

Su and coworkers reported a structural design following Murray's law. Structure with macro–meso–micropores shows high efficiency in transport (**Figure 21**).[83]

However, a postsynthesis method for building hierarchical structure shows less efficiency than that suggested by small-world models. The ideal long-range connection cannot be easily built, and some engineering problem including poor mechanical strength and surface coking would adversely influence the transport efficiency.

5. Perspective

Diffusion in zeolites is complicated. Collisional and random walk processes that lead to diffusion in zeolite channels are processes with low efficiency. In addition, deactivation occurs stochastically in zeolite cages, which leads to a pseudo-phase transition phenomenon, and efficiency is further severely decreased. Deactivation also leads to a decrease in total activity even when increasing the acid concentration at specific conditions. The deactivation process is revealed to be closely connected to the topology of the zeolite structure. These phenomena can be analyzed with a discrete Ising model.

Building a zeolite structure using guidelines from a small-world network model can give higher efficiency. A zeolite is comparable to a community in society with the property of a small-world network. At the angstrom level, water molecules can diffuse through aquaporin with ultrahigh efficiency. This is a superfast transport phenomenon that is due to the correct diameter and hydrophobic groups in aquaporin.[84,85] Quantum transport phenomena are also noticed over carbon nanotube and graphene.[86–88] Building long-range interconnections and nanochannels with quantum transportability will dramatically

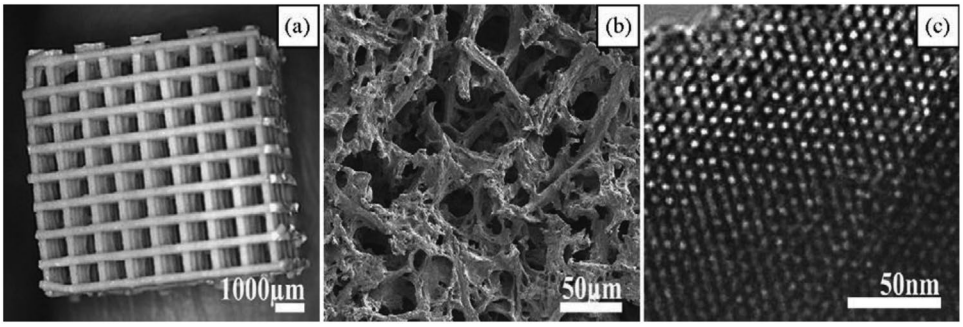

Figure 20. Hierarchical structure built on the multiscale. Reproduced with permission.[82] Copyright 2010, Elsevier B.V.

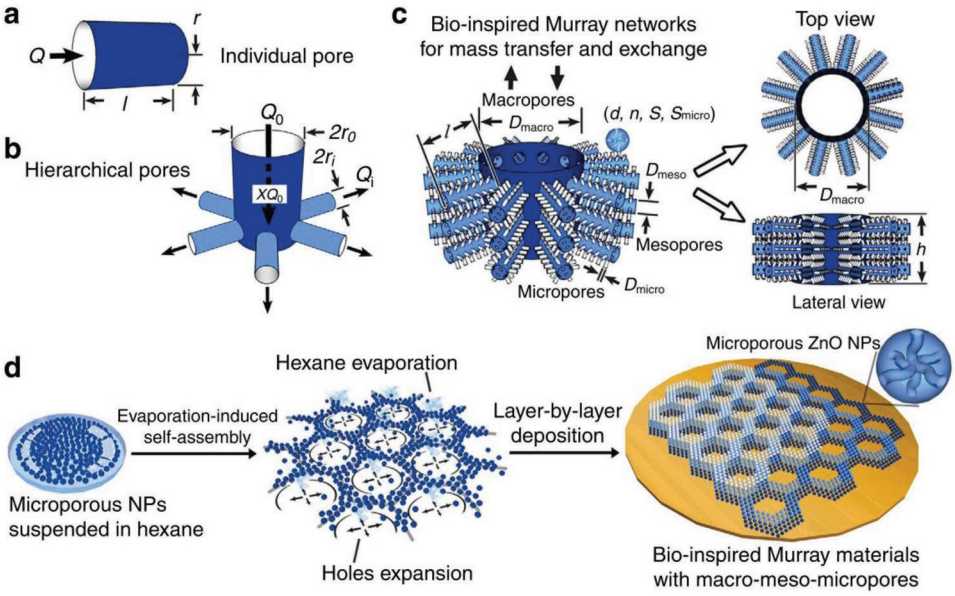

Figure 21. Hierarchical structure designed using Murray's law. Reproduced with permission.[83] Copyright 2017, Nature Publishing Group.

promote the overall transport efficiency. Graph theory can be applied to investigate the problem.

On a larger scale, a hierarchical structure is advantageous not only in zeolites but also in other fields. Besides its occurrence in zeolites, multiscale transport phenomena have been noted in other fields. E. g. at the meter level, the vascular system in mammals shows a hierarchical structure that follows Murray's law.[89,90] This hierarchical structure results in a 3/4 power scaling law relationship, indicating that there is a fourth dimension for life.[91] Full utilization of Murray's law and a high-dimensional concept will be beneficial for building a hierarchical network structure in zeolites.

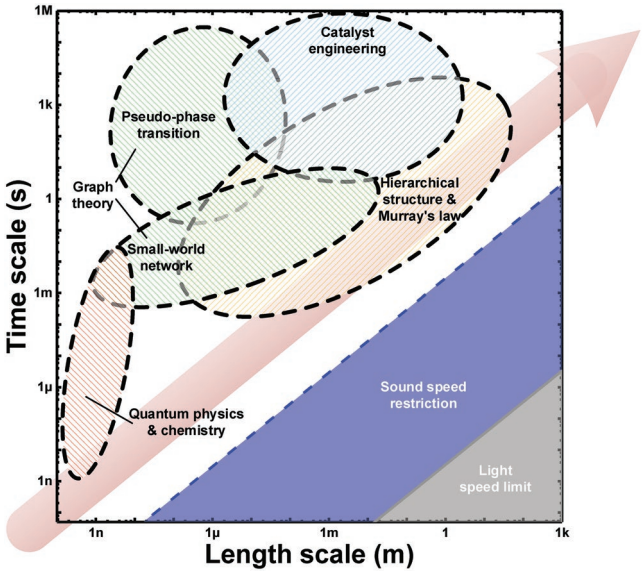

Figure 22. Connecting multiscale theory for modeling transport phenomena.

In the future, new comprehensive models and methods need to be developed. The introduction and use of a mechanism based on quantum physics and chemistry are essential. The building of quantum transport tunnels and designing a correct space confinement effect in a zeolite would help the synthesis of zeolites with superfast transport efficiency. The use of graph theory and discrete Ising models would help analyze it.

Long-range quantum transport research is still at an early stage and workers in the zeolite field have not yet paid it much attention, but the understanding of transport phenomena in zeolite channels from a quantum physics basis will bring a new horizon to zeolite research. On the macroscale where there is a negligible quantum effect, a hierarchical structure built using a postsynthesis method is effective. The problem of the self-organization of zeolite nanocrystals into hierarchical structures need to be studied. Small-world network and discrete models would perform as a bridge. The results of superfast transport from quantum physics and chemistry can be included as elemental steps in a graph theory model, and the optimization of the graph theory model can be applied to the design of the hierarchical structure. Here, there would be a chain of transport theories like that illustrated in **Figure 22**, and for the full understanding of the complex transport phenomena, an all-inclusive model would have to be assembled from the multiscale ones.

Acknowledgements

This work is supported by the National Natural Science Foundation of China (21908125) and the National Key Research and Development Program of China (2018YFB0604801). Besides, the authors also acknowledge the support from the China Postdoctoral Science Foundation (2019T120099), Tsinghua University Initiative Scientific Research Program (20183080009), and Beijing National Research Center For Information Science And Technology (also known as Tsinghua National Laboratory for Information Science and Technology).

Conflict of Interest

The authors declare no conflict of interest.

Keywords

graph theory, pseudo-phase transition, transport phenomena, zeolites

Received: April 20, 2019
Revised: July 16, 2019
Published online: August 29, 2019

[1] A. W. Chester, E. G. Derouane, *Zeolite Characterization and Catalysis*, Springer, Netherlands **2009**.
[2] J. Zhu, Y. Cui, Z. Nawaz, Y. Wang, F. Wei, *Chin. J. Chem. Eng.* **2010**, *18*, 979.
[3] H. Zhou, Y. Wang, F. Wei, D. Wang, Z. Wang, *Appl. Catal., A* **2008**, *341*, 112.
[4] P. Tian, Y. Wei, M. Ye, Z. Liu, *ACS Catal.* **2015**, *5*, 1922.
[5] O. H. J. Muhammad, E. K. T. Kam, *Catal. Today* **1997**, *38*, 85.
[6] R. H. Harding, A. W. Peters, J. R. D. Nee, *Appl. Catal., A* **2001**, *221*, 389.
[7] G. Centi, P. Ciambelli, S. Perathoner, P. Russo, *Catal. Today* **2002**, *75*, 3.
[8] R. J. Farrauto, R. M. Heck, *Catal. Today* **2000**, *55*, 179.
[9] J. N. Armor, *Appl. Catal., B* **1992**, *1*, 221.
[10] P. J. Bereciartua, Á. Cantín, A. Corma, J. L. Jordá, M. Palomino, F. Rey, S. Valencia, E. W. Corcoran, P. Kortunov, P. I. Ravikovitch, A. Burton, C. Yoon, Y. Wang, C. Paur, J. Guzman, A. R. Bishop, G. L. Casty, *Science* **2017**, *358*, 1068.
[11] R. T. Yang, *Gas Separation by Adsorption Processes*, Elsevier Ltd., Oxford, England, UK **1987**.
[12] M. Stöcker, *Microporous Mesoporous Mater.* **2005**, *82*, 257.
[13] J. Crank, *The Mathematics of Diffusion*, 2nd ed., Oxford University Press, Oxford, England, UK **1975**.
[14] M. Eic, D. M. Ruthven, *Zeolites* **1988**, *8*, 40.
[15] W. Niessen, H. G. Karge, *Microporous Mater.* **1993**, *1*, 1.
[16] H. G. Karge, W. Nießen, *Catal. Today* **1991**, *8*, 451.
[17] H. Jobic, D. N. Theodorou, *Microporous Mesoporous Mater.* **2007**, *102*, 21.
[18] H. Jobic, M. Bée, J. Caro, M. Bülow, J. Kärger, *J. Chem. Soc., Faraday Trans. 1* **1989**, *85*, 4201.
[19] F. Salles, H. Jobic, T. Devic, P. L. Llewellyn, C. Serre, G. Férey, G. Maurin, *ACS Nano* **2009**, *4*, 143.
[20] A. J. O'Malley, V. García Sakai, I. P. Silverwood, N. Dimitratos, S. F. Parker, C. R. A. Catlow, *Phys. Chem. Chem. Phys.* **2016**, *18*, 17294.
[21] J. G. Tsikoyiannis, J. Wei, *Chem. Eng. Sci.* **1991**, *46*, 255.
[22] R. Kolvenbach, L. F. Gonzalez Peña, A. Jentys, J. A. Lercher, *J. Phys. Chem. C* **2014**, *118*, 8424.
[23] D. Cai, Y. Cui, Z. Jia, Y. Wang, F. Wei, *Front. Chem. Sci. Eng.* **2018**, *12*, 77.
[24] M. Guisnet, P. Magnoux, *Appl. Catal.* **1989**, *54*, 1.
[25] F. C. Hendriks, S. Mohammadian, Z. Ristanović, S. Kalirai, F. Meirer, E. T. C. Vogt, P. C. A. Bruijnincx, H. C. Gerritsen, B. M. Weckhuysen, *Angew. Chem., Int. Ed.* **2018**, *57*, 257.
[26] B. M. Weckhuysen, F. Hendriks, J. Schmidt, J. Rombouts, K. Lammertsma, P. Bruijnincx, *Chem. - Eur. J.* **2017**, *23*, 6305.
[27] D. Fu, K. Park, G. Delen, Ö. Attila, F. Meirer, D. Nowak, S. Park, J. E. Schmidt, B. M. Weckhuysen, *Chem. Commun.* **2017**, *53*, 13012.
[28] F. C. Hendriks, F. Meirer, A. V. Kubarev, Z. Ristanović, M. B. J. Roeffaers, E. T. C. Vogt, P. C. A. Bruijnincx, B. M. Weckhuysen, *J. Am. Chem. Soc.* **2017**, *139*, 13632.
[29] J. E. Schmidt, J. D. Poplawsky, B. Mazumder, Ö. Attila, D. Fu, D. A. M. de Winter, F. Meirer, S. R. Bare, B. M. Weckhuysen, *Angew. Chem.* **2016**, *128*, 11339.
[30] D. Mores, J. Kornatowski, U. Olsbye, B. M. Weckhuysen, *Chem.-Eur. J.* **2011**, *17*, 2874.
[31] D. Mores, E. Stavitski, M. H. F. Kox, J. Kornatowski, U. Olsbye, B. M. Weckhuysen, *Chem. - Eur. J.* **2008**, *14*, 11320.
[32] M. H. F. Kox, E. Stavitski, J. C. Groen, J. Pérez-Ramírez, F. Kapteijn, B. M. Weckhuysen, *Chem. - Eur. J.* **2008**, *14*, 1718.
[33] B. M. Weckhuysen, *Angew. Chem., Int. Ed.* **2009**, *48*, 4910.
[34] J. Kärger, S. Vasenkov, S. M. Auerbach, *Handbook of Zeolite Science and Technology*, CRC Press, Boca Raton, Florida, USA **2003**, pp. 458–560.
[35] E. W. Thiele, *Ind. Eng. Chem.* **1939**, *31*, 916.
[36] P. B. Weisz, J. S. Hicks, *Chem. Eng. Sci.* **1962**, *17*, 265.
[37] A. O. E. Beyne, G. F. Froment, *Chem. Eng. Sci.* **1993**, *48*, 503.
[38] M. Sahimi, *AIChE J.* **1993**, *39*, 369.
[39] C. R. A. Catlow, C. M. Freeman, B. Vessal, S. M. Tomlinson, M. Leslie, *J. Chem. Soc., Faraday Trans.* **1991**, *87*, 1947.
[40] R. Krishna, J. M. van Baten, *Microporous Mesoporous Mater.* **2008**, *109*, 91.
[41] Y. Wang, C. Wang, B. Li, Z. Xie, *J. Energy Chem.* **2013**, *22*, 914.
[42] Z. Jia, D. Cai, Y. Cui, W. Qian, F. Wei, *Catal. Today* **2018**, *301*, 244.
[43] B. Smit, T. L. M. Maesen, *Chem. Rev.* **2008**, *108*, 4125.
[44] J. Kaerger, *J. Phys. Chem.* **1991**, *95*, 5558.
[45] T. Titze, A. Lauerer, L. Heinke, C. Chmelik, N. E. R. Zimmermann, F. J. Keil, D. M. Ruthven, J. Kärger, *Angew. Chem., Int. Ed.* **2015**, *54*, 14580.
[46] J. Kärger, D. M. Ruthven, *New J. Chem.* **2016**, *40*, 4027.
[47] J. Kärger, *ChemPhysChem* **2015**, *16*, 24.
[48] A. V. Barzykin, S. Hashimoto, *J. Chem. Phys.* **2000**, *113*, 2841.
[49] D. M. Smith, *AIChE J.* **1986**, *32*, 329.
[50] X. Guo, Z. Liu, B. Zhong, *Microporous Mesoporous Mater.* **1998**, *23*, 203.
[51] R. Mann, H. Golshan, *Chem. Eng. Commun.* **1981**, *12*, 377.
[52] P. Erdos, A. Renyi, *Publ. Math. Inst. Hung. Acad. Sci.* **1960**, *5*, 17.
[53] P. Erdos, A. Renyi, *Publ. Math. Debrecen* **1959**, *6*, 290.
[54] C. Moore, M. E. J. Newman, *Phys. Rev. E* **2000**, *61*, 5678.
[55] D. Chen, H. P. Rebo, A. Holmen, *Chem. Eng. Sci.* **1999**, *54*, 3465.
[56] G. R. Grimmett, S. L. G. R. Grimmett, S. S. Chern, B. Eckmann, H. Hironaka, *Percolation*, Springer, Berlin/Heidelberg, Germany **1999**.
[57] H. Kesten, *Percolation Theory for Mathematicians*, Vol. *423*, Springer, Berlin/Heidelberg, Germany **1982**.
[58] D. Cai, Y. Ma, Y. Hou, Y. Cui, Z. Jia, C. Zhang, Y. Wang, F. Wei, *Catal. Sci. Technol.* **2017**, *7*, 2440.
[59] R. B. LaPierre, A. C. Rohrman, J. L. Schlenker, J. D. Wood, M. K. Rubin, W. J. Rohrbaugh, *Zeolites* **1985**, *5*, 346.
[60] Y. Hou, N. Wang, J. Zhang, W. Qian, *RSC Adv.* **2017**, *7*, 14309.
[61] D. Cai, Y. Hou, C. Zhang, N. Wang, Z. Chen, W. Song, Z. Jia, Y. Wang, W. Qian, F. Wei, *Nanoscale* **2018**, *10*, 16431.
[62] V. Latora, M. Marchiori, *Phys. Rev. Lett.* **2001**, *87*, 198701.
[63] D. J. Watts, S. H. Strogatz, *Nature* **1998**, *393*, 440.
[64] M. Choi, K. Na, J. Kim, Y. Sakamoto, O. Terasaki, R. Ryoo, *Nature* **2009**, *461*, 246.
[65] K. Na, C. Jo, J. Kim, K. Cho, J. Jung, Y. Seo, R. J. Messinger, B. F. Chmelka, R. Ryoo, *Science* **2011**, *333*, 328.
[66] Y. Liu, X. Zhou, X. Pang, Y. Jin, X. Meng, X. Zheng, X. Gao, F. Xiao, *ChemCatChem* **2013**, *5*, 1517.

[67] X. Meng, F. Xiao, *Chem. Rev.* **2013**, *114*, 1521.
[68] Y. Ma, D. Cai, Y. Li, N. Wang, U. Muhammad, A. Carlsson, D. Tang, W. Qian, Y. Wang, D. Su, F. Wei, *RSC Adv.* **2016**, *6*, 74797.
[69] Z. P. Lai, G. Bonilla, I. Diaz, J. G. Nery, K. Sujaoti, M. A. Amat, E. Kokkoli, O. Terasaki, R. W. Thompson, M. Tsapatsis, D. G. Vlachos, *Science* **2003**, *300*, 456.
[70] E. M. Gallego, M. T. Portilla, C. Paris, A. Leon-Escamilla, M. Boronat, M. Moliner, A. Corma, *Science* **2017**, *355*, 1051.
[71] Y. Cui, Q. Zhang, J. He, Y. Wang, F. Wei, *Particuology* **2013**, *11*, 468.
[72] K. Shen, L. Zhang, X. Chen, L. Liu, D. Zhang, Y. Han, J. Chen, J. Long, R. Luque, Y. Li, B. Chen, *Science* **2018**, *359*, 206.
[73] K. Shen, W. Qian, N. Wang, C. Su, F. Wei, *J. Am. Chem. Soc.* **2013**, *135*, 15322.
[74] N. Wang, W. Qian, K. Shen, C. Su, F. Wei, *Chem. Commun.* **2016**, *52*, 2011.
[75] Y. Song, C. Sun, W. Shen, L. Lin, *Appl. Catal., A* **2007**, *317*, 266.
[76] R. Otomo, U. Müller, M. Feyen, B. Yilmaz, X. Meng, F. Xiao, H. Gies, X. Bao, W. Zhang, D. De Vos, T. Yokoi, *Catal. Sci. Technol.* **2016**, *6*, 713.
[77] W. Wan, T. Fu, R. Qi, J. Shao, Z. Li, *Ind. Eng. Chem. Res.* **2016**, *55*, 13040.
[78] M. Bjørgen, F. Joensen, M. Spangsberg Holm, U. Olsbye, K. Lillerud, S. Svelle, *Appl. Catal., A* **2008**, *345*, 43.
[79] M. Li, Y. Zhou, C. Ju, Y. Fang, *Appl. Catal. A* **2016**, *512*, 1.
[80] S. Mitchell, M. Boltz, J. Liu, J. Pérez-Ramírez, *Catal. Sci. Technol.* **2017**, *7*, 64.
[81] Z. Qin, G. Melinte, J. Gilson, M. Jaber, K. Bozhilov, P. Boullay, S. Mintova, O. Ersen, V. Valtchev, *Angew. Chem., Int. Ed.* **2016**, *55*, 15049.
[82] B. Louis, F. Ocampo, H. S. Yun, J. P. Tessonnier, M. M. Pereira, *Chem. Eng. J.* **2010**, *161*, 397.
[83] X. Zheng, G. Shen, C. Wang, Y. Li, D. Dunphy, T. Hasan, C. J. Brinker, B. Su, *Nat. Commun.* **2017**, *8*, 14921.
[84] J. B. Heymann, A. Engel, P. Agre, K. Mitsuoka, K. Murata, T. Hirai, T. Walz, Y. Fujiyoshi, *Nature* **2000**, *407*, 599.
[85] H. Sui, B. Han, J. K. Lee, P. Walian, B. K. Jap, *Nature* **2001**, *414*, 872.
[86] W. Bao, L. Jing, J. Velasco, Y. Lee, G. Liu, D. Tran, B. Standley, M. Aykol, S. B. Cronin, D. Smirnov, M. Koshino, E. McCann, M. Bockrath, C. N. Lau, *Nat. Phys.* **2011**, *7*, 948.
[87] E. A. Laird, F. Kuemmeth, G. A. Steele, K. Grove-Rasmussen, J. Nygård, K. Flensberg, L. P. Kouwenhoven, *Rev. Mod. Phys.* **2015**, *87*, 703.
[88] S. J. Tans, M. H. Devoret, H. Dai, A. Thess, R. E. Smalley, L. J. Geerligs, C. Dekker, *Nature* **1997**, *386*, 474.
[89] C. D. Murray, *Proc. Natl. Acad. Sci. USA* **1926**, *12*, 207.
[90] C. D. Murray, *J. Gen. Physiol.* **1927**, *10*, 725.
[91] G. B. West, *Science* **1999**, *284*, 1677.